An evaluation of the temperature dependence of cohesive properties for two structural epoxy adhesives

Tomas Walander [1,a] Anders Biel [1,b] and Ulf Stigh [1,c]

[1] University of Skövde, P.O. Box 408, SE-541 28 Skövde, SWEDEN

[a] tomas.walander@his.se, [b] anders.biel@his.se, [c] ulf.stigh@his.se

Keywords: Double cantilever beam, End notched flexure, Fracture energy, Kruskal-Wallis test, Peak stress, Regression analyses.

Abstract.
Cohesive modelling provides a more detailed understanding of the fracture properties of adhesive joints than provided by linear elastic fracture mechanics. A cohesive model is characterized by a stress-deformation relation of the adhesive layer. This relation can be measured experimentally. Two parameters of the stress-deformation relation are of special importance; the area under the curve, which equals the fracture energy, and the peak stress. The influence of temperature of these parameters is analyses experimentally and evaluated statistically for two structural epoxy adhesives in the span from of -40°C to +80°C. The adhesives are used by the automotive industry and a temperature span below the glass transition temperature is considered. The results show that that temperature has a modest influence on the adhesives Mode I fracture energy. For one of the adhesives, the fracture energy is independent of the temperature in the evaluated temperature span. In mode II, the influence of temperature is larger. The peak stresses decreases almost linearly with an increasing temperature in both loading cases and for both adhesives.

Introduction

The automotive industries are striving to minimize the weight of their products in order to reduce the fuel consumption and thereby the emissions. In addition, the manufacturers are facing requirements to improve the crashworthiness. This is often at the expense of an increased weight. By using lightweight materials such as aluminium or composites in the body structure and combine these with tough material, e.g. steel, at impact zones, a more optimized solution can be obtained. Today, the majority of body structures consist of alloyed steel sheets that are joined by spot welds. A disadvantage with spot welds is the difficulty to join steel with aluminium alloys. This has put focus on modern crash resistant epoxy adhesives that enable joining of dissimilar materials. When using adhesives in a body structure it is in terms of crashworthiness required that the adhesive layers remain intact during a crash. This secures that bonded material deform in a predicted mode to dissipate the kinetic energy safely.

With cohesive modelling, a stress-deformation relation is used to characterize the strength of an adhesive layer. This is a constitutive relation on a structural length scale between the traction exerted on the interfaces of the adhesive to the adherends and the separation of the interfaces. The separation equals the deformation of the adhesive layer. In the sequel, this relation is denoted a stress-deformation law. Fig. 1 indicates peel and shear deformation. These are characterized by peel deformation, w, and peel stress, σ; and shear deformation, v, and shear stress, τ. The success of this characterization is due to the high toughness of modern adhesives. With brittle adhesives, we can expect to have to model the details of the fields more accurately.

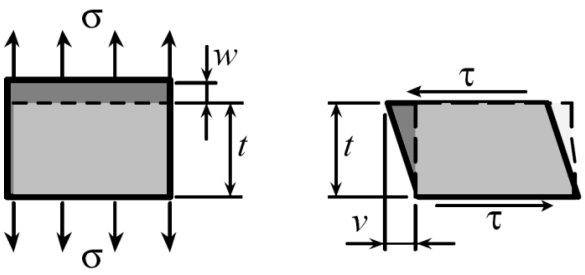

Fig.1. Deformation modes with corresponding stress and deformation of an adhesive layer with initial thickness *t*. *Left*: Mode I, peel. *Right*: Mode II, shear.

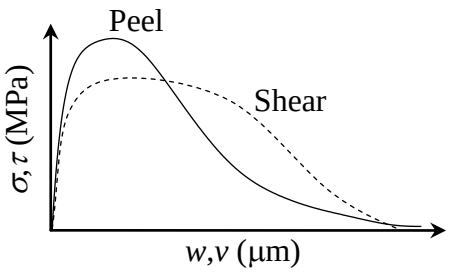

Fig.2. Stress-deformation relations for an adhesive layer.

The strength of adhesively bonded multi-material build-up structures can be adequately predicted using cohesive modelling and the finite element method, cf. e.g. [1]. This modelling provides a more detailed understanding of the fracture properties of adhesive joints than can be achieved with fracture mechanics. Methods to measure the cohesive properties in Mode I, II and in mixed mode loading are summarized in [2]. Typical stress-deformation relations are shown in Fig. 2. Two parameters of these relations are of special importance; the area under each curve which equals the fracture energy and the peak stress.

An automotive body structure is required to fulfil its requirements at all working temperatures. The relevant areas of a car body for which adhesives are of interest normally suffers the temperature range -40°C $\leq T \leq$ 80°C. Some studies of the influence of temperature have been performed. In [3] it is shown that the stress-deformation relation for the epoxy adhesive DOW Betamate XW 1044-3 (DB1044) is strongly temperature dependent in Mode I. In this study, the entire stress-deformation law is evaluated at seven equally distributed temperatures with ten repeated experiments at each temperature. In [4] it is shown that the fracture energy for an structural epoxy adhesive decreases in the temperature region $0.7 < T / T_g < 1.0$, where T_g denotes the glass transition temperature. For most epoxies it is about 100°C. Furthermore, it is shown that the yield strength decreases with increasing temperature and increases with increasing strain rate. In [4], the fracture energy is determined using an unstable specimen and the experiments are evaluated using linear elastic fracture mechanics (LEFM). That is, the entire cohesive relation is not captured.

Cohesive models are implemented in finite element software to simulate the behaviour of adhesively joined structures. To perform these analyses considering temperature, the temperature dependence of the adhesive layer has to be taken into account. The previous studies do not provide all the necessary data and therefor a cohesive model cannot yet be established. This implies that new experiments need to be performed. An adhesive that is of current interest by the automotive industry is the crash resistant epoxy SikaPower498 (SP498). In this work, temperature studies are performed on this adhesive in Mode I and Mode II. Statistical methods are used to evaluate the influence of temperature on the two important parameters, peak stress and fracture energy. Moreover, the results in [3] are re-evaluated using statistical methods.

Methods

The two most frequently used test specimens to measure Mode I and Mode II fracture properties for adhesives are the double cantilever beam (DCB) and the end notched flexure specimen (ENF) cf. Figs. 3 and 4, respectively. These specimens are used in the studies in [3] and [4]. The specimens

each consist of two adherends that are partially joined by an adhesive layer. The part of the specimens that is not joined by an adhesive layer is considered as a crack, and the start of the adhesive layer is denoted the crack tip.

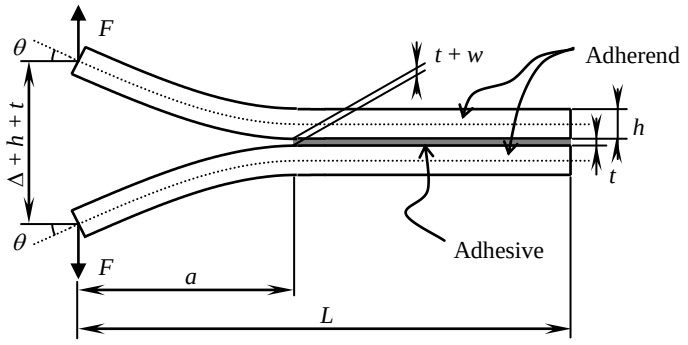

Fig.3. Deformed DCB test specimen with out of plane width *b*.

For the DCB specimen the adherends are separated by a prescribed deformation Δ and the reaction force, *F*, is measured. The stress-deformation relation for the DCB specimen is given by Eq. 1 in which *J* is derived either by using beam theory, cf. [5], or by using the path independent *J*-integral, cf. [6].

$$\sigma(w) = \frac{\mathrm{d}J}{\mathrm{d}w} \equiv \frac{\mathrm{d}}{\mathrm{d}w}\left(\frac{2F\sin\theta}{b}\right), \tag{1}$$

where, θ is the rotation of the loading points and *b* is the specimen width.

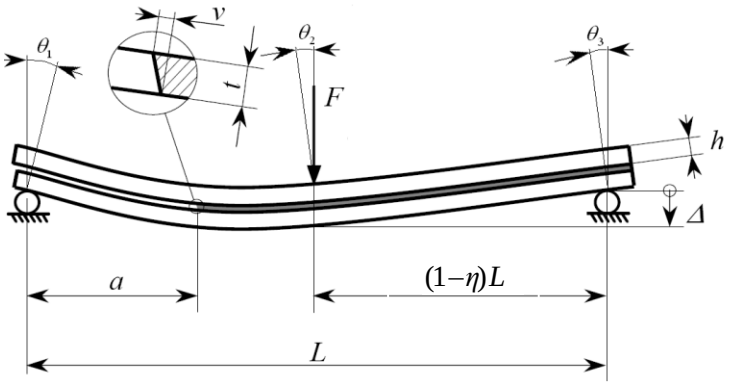

Fig.4. Deformed ENF test specimen with out of plane width *b*.

A properly designed ENF-specimen gives almost a state of pure shear at the crack tip. A recently developed method to measure *J* for the ENF specimen is presented in [7] and is validated showing good agreement to input data using finite element analysis in [8]. From this method the stress-deformation relation of the adhesive layer is given as

$$\tau(v) = \frac{\mathrm{d}J}{\mathrm{d}v} \equiv \frac{\mathrm{d}}{\mathrm{d}v}\left\{\frac{F}{b}\left[(1-\eta)\sin\theta_1 - \sin\theta_2 + \eta\sin\theta_3\right]\right\} \tag{2}$$

where F denotes the load, η is the distance between the left support and the loading point, b is the specimen width and θ_1, θ_2 and θ_3 are the rotations at the three supports. These are considered positive when increasing clockwise, cf. Fig. 4. Eqs. 1 and 2 provide the entire stress-deformation relation of the adhesive layer for each mode, respectively. In neither of these methods the constitutive properties of the adherends need to be known. Furthermore, both methods allow for plastic deformation of the adherends as long as no unloading from a plastic state takes place. Unloading from a plastic state would invalidate the path-independence of the J-integral used to derive Eqs. 1 and 2.

Regression analysis is used to evaluate the temperature dependence of the peak stress and the fracture energy; collectively denoted response variables, y. Simple models for the influence of the explanatory variable x_1 are given by a linear and a second order model, i.e.

$$y = x_1\beta_1 + \beta_0 + \varepsilon. \qquad y = x_1^2\beta_2 + x_1\beta_1 + \beta_0 + \varepsilon. \qquad \text{(3a, b)}$$

In this study, the only explanatory variable is the temperature; ε is often denoted the disturbance term. The parameters β_2, β_1 and β_0 are to be estimated using the least square method. A major assumption in this method is that the explanatory variable is measured without errors. That is, the temperature is assumed to be measured exactly. If the influence of both $|\beta_2|$ and $|\beta_1|$ is small, the response variable is considered independent of the explanatory variable. The coefficient of determination R^2 is often used to indicate if the fit is good; if R^2 equals 1, all data points are on the fitted curve. On the other hand, if there is no dependence of the response variable on the explanatory variable, R^2 equals zero cf. e.g. [9].

Another way of analysing dependence, not assuming a normal distribution, is to use a non-parametric rank test such as the Kruskal-Wallis test, cf. [10]. This one-way analysis of variance of ranks enables testing several populations against each other. If the number of samples of each population is large enough, a certain test variable K can be assumed to be chi-square, χ^2-distributed. If $K < \chi^2_{g-1}$ the medians of each population are assumed equal. The value χ^2_{g-1} is determined to give a certain probability. Thus, indicating that there is no dependence of the explanatory variable. The procedure and notation is described below. All observations are first ranked independent of the temperature. That is, the smallest value is given the rank 1; the second smallest is given the rank 2 and so on until the largest value is given the rank n equal to the total number of observations. All observations are then grouped in samples corresponding to the temperature. This gives g samples corresponding to the g temperatures. In each group, the average rank of the observations in each group is calculated, $\bar{r}_i$, where $i = 1,2,\ldots g$. With n_i equal to the number of observations in sample i, the test variable K is calculated according to

$$K = \frac{12}{n(n+1)}\sum_{i=1}^{g} n_i \bar{r}_i^{\,2} - 3(n+1) \qquad (4)$$

Using a table of the χ^2_{g-1}-distribution, the probability that the medians are equal is estimated. More formally, the null hypothesis that there is no difference in the response variable between the samples is rejected if $K \geq \chi^2_{g-1}$. With a 5 % risk of rejecting the null hypothesis even if it is true, we need K smaller than 9.49 with five evaluated temperatures; with seven evaluated temperature we need K smaller than 12.59. This risk is denoted the level of significance.

Experiments

Two experimental set-ups for the performed experiments are shown in Fig. 5. Here, the climate chambers are not shown. With the DCB testing machine, two crossheads are separating the load points on both sides with a prescribed loading rate, $\dot{\Delta} = 10\,\mu$m/s. This is slow enough to consider the test quasi-static. In these experiments, the crack tip separation, w, as well as the load point displacement, Δ, are measured using linear variable differential transformers (LVDT). The rotation of the loading point, θ, is measured using an incremental shaft encoder and the load, F, is measured using a load cell. Only the rotation of one of the adherends is measured and it is assumed that the specimen deform symmetrically. This assumption has been tested in earlier experiments and found to give sufficient accuracy. An external climate chamber is used for the temperature span -40°C $\leq T \leq$ 80°C. The experiments are performance identically as in [3] with exception for the number of evaluated temperature intervals.

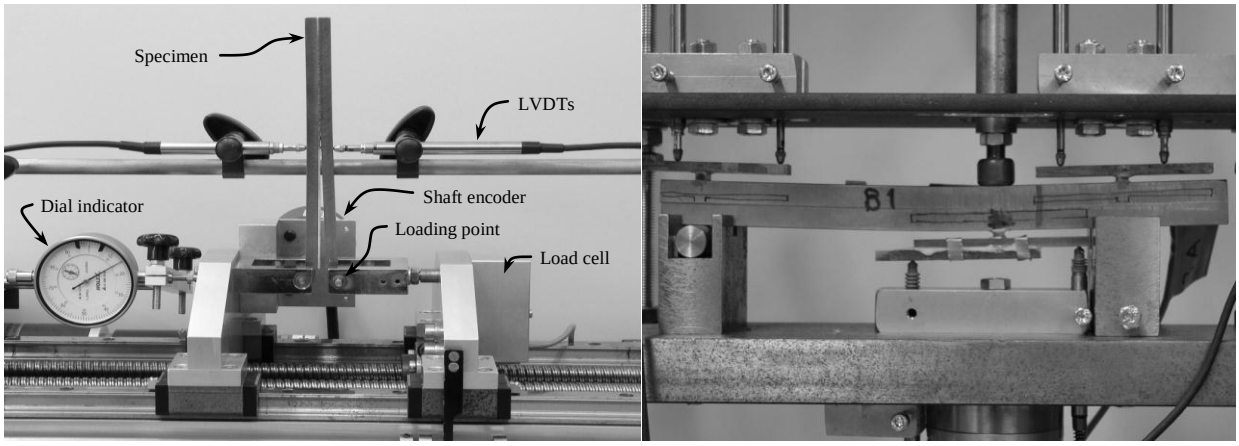

Fig.5. Experimental set-ups with deformed specimens. *Left*: DCB test rig. *Right*: ENF test rig.

For the ENF set-up, a servo hydraulic test machine is used. The load acts at $\eta = 0.7$, cf. Fig. 4 and 5. Two LVDTs for measurements of each rotations, θ_i, and one LVDT for measuring the shear deformation, v, are used. The load point displacement, Δ, is also here given a prescribed loading rate, $\dot{\Delta} = 3.8\mu$m/s, slow enough to be considered the test as quasi-static. The aim is to test the adhesive at the same temperatures as in the DCB-experiments. However, the climate chamber has a lower limit of -30 °C. Thus, -30 °C is the lowest evaluated temperature for the ENF experiments.

The adherends of the specimens are made of the Uddeholm Rigor tooling steel that, according to tensile tests, allows for engineering strains up to 14 % before plastic straining start, cf. [8]. The thickness of the adhesive layer is nominally t = 0.3 mm for all specimens with SP498 and t = 0.2 mm for the DB1044 adhesive. The DCB specimens has the dimensions in mm, L = 160, a = 80, h = 6.5 and b = 5, cf. Fig. 3. The ENF specimens has the dimensions in mm L = 200, a = 70, h = 10 and b = 10, cf. Fig. 4. In order for the J-integral to be valid the stresses in the adhesive layer at the right end of the specimen, cf. Fig. 4, needs to be negligible. Therefor an overhang of 50 mm is used for the ENF specimens, cf. Fig. 5. Also in order to ensure that the ENF specimen remain on the support during deformation, an overhang of 20 mm is used on the left end. This gives the total specimen length of 270 mm.

Evaluation and results

From the experiments, stress-deformation relations like the ones in Fig. 2 are obtained using Eqs. 1 and 2. For each experiment, the two parameters fracture energy, J_c, and the peak stress, are presented in Fig. 6. The results of the DB1044 adhesive in [3] are also included in this evaluation. The DB1044 adhesive have significant lower fracture energies than the SP498 adhesive. During manufacturing of the specimens, air bubbles may arise in the adhesive layer. In order to justly be able to compare two different adhesives, all specimens are carefully investigated after the experiments. If an adhesive layer contains air bubbles in the region close to the crack tip, it is excluded from the evaluation since it affects the measured fracture energy.

From Fig. 6 it is concluded that the peak stresses decrease with an increase in temperature for both adhesives, both in Mode I and in Mode II. Regarding the fracture energy, indications that the fracture energy is independent of temperature in Mode I are given in Fig. 6. This result is however not observed in Mode II where the fracture energy clearly decreases at temperatures above 50°C which corresponds with the observation in [4].

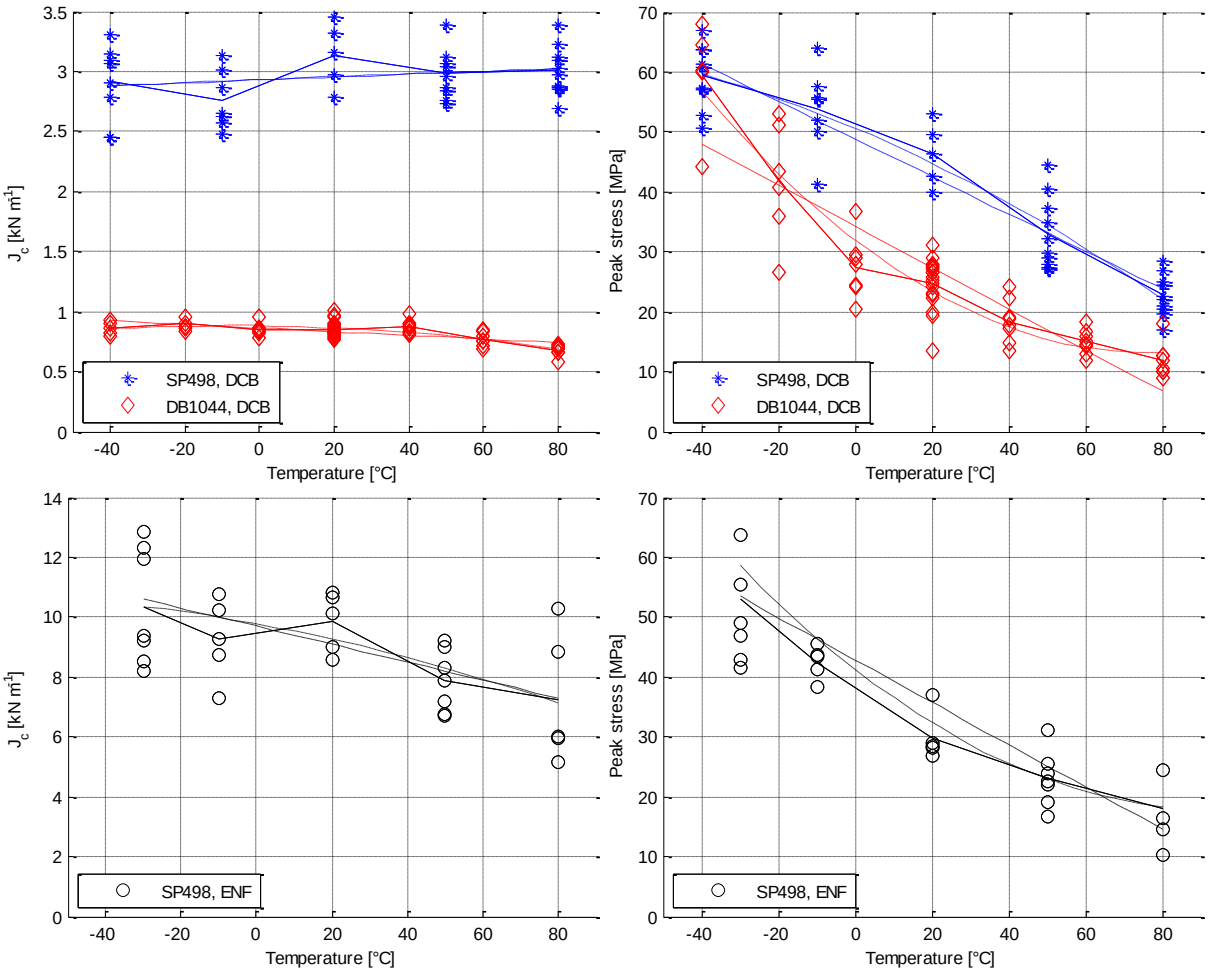

Fig.6. Experimental results. *Top*: Mode I loading. *Bottom*: Mode II loading. *Left*: Fracture energy. *Right*: Peak stress. The solid lines combine the mean value of each temperature group. The dashed and the dashed-dotted lines show the results of a first and a second order regression analysis, respectively.

By performing regression analyses, the estimated trend with respect to the temperature are calculated by the least square method, cf. Fig. 6. The estimated coefficients of regression in Eq. 3a and Eq. 3b are presented in Table 1 where the temperature in centigrade has been used.

Mode I. The top graphs in Fig. 6 show the results from Mode I loading. As shown, the first and second order regression curves virtually coincide for the fracture energy of both adhesives. For SP498 R^2 is very small indicating that there is no dependence of the temperature on the fracture energy. This is supported by K = 6.04 in the Kruskal-Wallis test at the 5 % level of significance. Thus, it is safe to state that the fracture energy in Mode I does not depend on the temperature in the tested interval. For DB1044, there is a slight influence of the temperature. We get K = 31.2 and would have needed a value below 12.59 with the present level of significance. The mean values of the Mode I fracture energies are μ_{SP498} = 2.68 kN m^{-1} and μ_{DB1044} = 825 N m^{-1} for the SP498 and the DB1044 adhesive, respectively.

The peak stresses decreases with increasing temperature. For SP498, a linear regression curve gives a good fit; for DB1044 a parable fit the data accurately, both with R^2 values near 0.9.

Mode II. The bottom graphs in Fig. 6 shows the results from Mode II loading for SP498. The fracture energy as well as the peak stress cannot be considered as temperature independent. The Kruskal-Wallis test gives K = 10.3 and a value below 9.49 would be necessary with the 5 % level of significance. The second order regression analysis predicts a continuous decrease in fracture energy with respect to the temperature. However, with a small R^2 value (0.35). Both a linear and a second order regression curve give high R^2 values for the peak stress.

Table 1. Estimated coefficients of regression and test value, K.

		Peak stress				Fracture energy, J_c					
		β_2 [kPa °C^{-2}]	β_1 [kPa °C^{-1}]	β_0 [MPa]	R^2 [-]	K [-]	β_2 [mN m^{-1} °C^{-2}]	β_1 [N m^{-1} °C^{-1}]	β_0 [kN m^{-1}]	R^2 [-]	
Mode I	DB1044	3.19	-491	32.0	0.85	31.2	-25.3	0.37	0.88	0.55	a)
		-	-345	34.3	0.76		-	-1.53	0.86	0.39	b)
	SP498	-1.08	-270	50.6	0.88	6.04	-1.91	1.28	2.93	0.05	a)
		-	-312	48.8	0.87		-	1.21	2.93	0.05	b)
Mode II		-2.24	-426	38.1	0.82	10.3	-0.10	-22.8	9.62	0.35	a)
		-	-325	40.5	0.78		-	-27.4	9.50	0.35	b)

a) Second order regression analysis b) Linear regression analysis

It is also interesting to note that the linear models for all peak stresses have about the same slope, i.e. β_1 varies from about -310 to -350 kPa °C^{-1}.

Conclusions

Within the evaluated temperature interval, -40 ≤ T ≤ 80 °C, the evaluation show a temperature independent Mode I fracture energy for SP498. For DB1044, there is a small influence of the temperature in Mode I. However, the influence is so small that it is reasonable to ignore the influence for engineering purposes. There is an influence of the temperature on the fracture energy in Mode II with a decrease in fracture energy with an increase in temperatures. The peak stresses

decreases almost linearly with increasing temperature for both epoxy adhesives and for both Mode I and II for SP498.

Acknowledgements
This work is funded by Swedish Knowledge Foundation through the MASLIM project. The author wish to thank Dr Thomas Carlberger for providing experimental results, SAAB Automobile AB, for providing a climate chamber for the DCB experiments and Mr Gunnar Åkerström at Volvo Material Technology for help in performing the ENF-experiments. Also thanks to those who have helped with finding appropriate statistical methods for this work, Mr Magnus Bredberg and Mrs Marie Lundgren at the School of Technology and Society at the University of Skövde.

References
[1] T. Carlberger, U. Stigh: Thin-Wall. Str. Vol. 48 (2010) p. 609
[2] U. Stigh, K.S. Alfredsson, T. Andersson, A. Biel, T. Carlberger, K. Salomonsson: Int. J. Fract. Vol. 165 (2010), p. 149
[3] T. Carlberger, A. Biel, U. Stigh: Int. J. Fract. Vol. 155 (2009) p. 155
[4] H. Chai: Int. J. Fract. Vol. 119 (2004) p. 25
[5] T. Andersson, U. Stigh: Int. J. Sol. Struct. (2004) Vol. 41, p. 413
[6] P. Olsson, U. Stigh: Int. J. Fract. Vol. 41 (1988) p. R71
[7] U. Stigh, K.S. Alfredsson, A. Biel, in: Proceedings IMECE2009 (2009).
[8] T. Walander: *System for measurement of cohesive laws* (MSc thesis University of Skövde, 2009)
[9] R. A. Johnson, S. W. Wichern: *Applied multivariate statistical analysis*, 3rd ed. (Prentice Hall 1992)
[10] W.H. Kruskal, W. A. Wallis: J. Am. Stat. Assoc. Vol. 47 (1952) p. 583